

# 2D APODIZATION IN UWB SAR USING LINEAR FILTERING

Thomas K. Sjögren, Viet T. Vu and Mats I. Pettersson

Department of Electrical Engineering  
Blekinge Institute of Technology (BTH)

## ABSTRACT

In this paper, an investigation is made on how sidelobes can be suppressed in ultrawideband-ultrawidebeam (UWB) Synthetic Aperture Radar (SAR) using apodization. Due to the special properties of UWB SAR such as very wide integration angle and very large relative bandwidth, the support for the spectrum of a SAR image differs distinctively from a rectangle, which is the normal approximation in narrowband-narrowbeam (NB) SAR. The proposal in the paper is to apply non-separable windows to the spectrum, in order to suppress sidelobes. Non-separable windows are shown to give less broadening of mainlobe while maintaining the same suppression of sidelobes in comparison to separable windows. In the comparison, parameters for three different SAR systems are used.

**Index Terms**— Synthetic Aperture Radar, Apodization, Windowing, Signal Processing, UWB SAR.

## 1. INTRODUCTION

In remote sensing of for instance Earth, it is always desired to obtain clear images with good resolution. When forming images using Synthetic Aperture Radar (SAR) systems, there will always be sidelobes appearing in the images. The sidelobes may severely distort the images even though the resolution is very good. The sidelobes makes it hard to distinguish weak objects close to an object that gives very strong reflections. The reason is that the sidelobes of the strong reflecting object will be higher than the main lobe of the weaker objects. For this reason it is of interest to keep the sidelobes as low as possible.

Traditionally in SAR, apodization techniques are used in order to suppress sidelobes. This is done by applying windows either to the spectrum of raw data in fast time and slow time, or on the spectrum of SAR images[1-4]. The used windows are normally chosen to be separable[5]. Applying different windows, the sidelobes in azimuth and slant range can be controlled, and traded against loss in resolution. In the case of wide integration angles and large relative bandwidth, the support of the spectrum of neither the image, nor the raw data is of rectangular shape. Systems with large integration angle and large relative bandwidth are here denoted ultrawideband-ultrawidebeam (UWB) SAR

systems. In [1] and [4], separable windows were used on UWB SAR data. Applying non-separable windows may improve sidelobe suppression ability as the support of the spectrum no longer is of rectangular shape. Furthermore, in [1] and [4] the suppression of sidelobes was made using non-linear methods. Such methods have the advantage of suppressing sidelobes, while maintaining the same resolution. However, it may be hard to know what the relation between the apodized imaged and the original image is, with regard to the properties of the objects in the image. In [3] it is found that for an image apodized with one specific non-linear method, Spatially Variant Apodization (SVA), the estimation and classification ability is clearly degraded in comparison to using the original image. For this reason, it may be of interest to investigate how to suppress sidelobes and maintain good resolution using linear apodization. Furthermore, it is especially of interest to relate it to UWB SAR where not much research on linear apodization has been made.

In this paper, the ability of sidelobe suppression for non-separable windows is investigated and compared with separable windows. The comparison is made using parameters according to three different SAR systems as well as with different windows. The paper is organized as follows: section 2 introduces the sidelobe suppression methods, section 3 provides results of applying the methods for parameters corresponding to three different systems and section 4 concludes the paper.

## 2. SIDELOBE SUPPRESSION METHODS

In order to suppress sidelobes in SAR images, windows can, as mentioned in the last section, e.g. be applied in the wave domain of SAR images. In this paper, separable and non-separable windows are evaluated. In both cases, Bartlett and Hamming windows are used. The definition of separable window in this paper is given by a window that is a product of two windows, each being function of only  $k_x$  or only  $k_y$ . Such can of windows are described by (1).

$$W_{sep}(k_x, k_y) = W_{k_x} \left( \frac{k_x}{2k_c \sin\left(\frac{\phi_0}{2}\right)} \right) \cdot W_{k_y} \left( \frac{k_y - k_c}{k_{\max} - k_{\min}} \right) \quad (1)$$

where  $k_x$  and  $k_y$  denote wavenumber in azimuth and slant range direction respectively,  $k_c$  is wavenumber corresponding to centre frequency of the radar signal,  $\phi_0$  integration angle of the system,  $k_{max}$  and  $k_{min}$  maximum and minimum wavenumber of the radar signal.

A non-separable window, on contrary is interpreted as a window that is not a product of two windows that is each a function of only  $k_x$  and  $k_y$ . However, in this paper we restrict ourselves and use the name non-separable windows for windows described by (2) only.

$$W_{non-sep}(k_x, k_y) = W_\phi \left( \frac{\text{atan}\left(\frac{k_x}{k_y}\right)}{\frac{\phi_0}{2}} \right) \cdot W_{k_r} \left( \frac{\sqrt{k_x^2 + k_y^2} - k_c}{k_{max} - k_{min}} \right) \quad (2)$$

Inspecting (2), it can be understood that  $W_{non-sep}$  is a window which is a product of one window as a function of  $\phi$  and one window as a function of  $k_r$ . To have a better understanding of how the SAR spectrum in wave-domain looks, an illustration is shown in Fig. 1, in which the parameters used in (1) and (2) can be found.

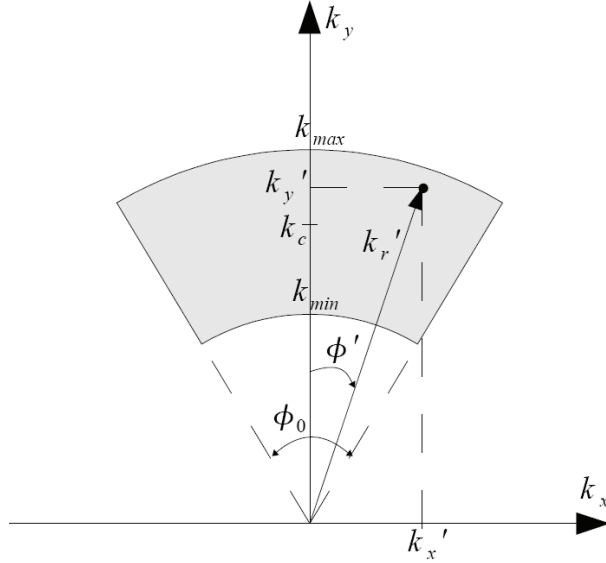


Fig. 1 Support of SAR spectrum in wave-domain. The parameters  $\phi_0$  and  $k_c$  are integration angle and centre wavelength of a SAR system. The fractional bandwidth,  $B_r$  is given by  $B_r = (k_{max} - k_{min}) / k_c$ , where  $k_{max}$  and  $k_{min}$  are the wavenumbers corresponding to the highest and the lowest signal frequencies. For an arbitrary point in the spectrum,  $(k'_x, k'_y)$ , a change of variable to  $(\phi', k'_r)$  can be obtained by  $(\phi', k'_r) = (\text{atan}(k'_x / k'_y), \sqrt{k_x^2 + k_y^2})$ .

TABLE I  
SYSTEM PARAMETERS FOR EVALUATIONS OF SIDELOBE SUPPRESSION

System	$\Phi_0$ (degrees)	$B_r$
A	30	0.25
B	90	0.25
C	140	1.2

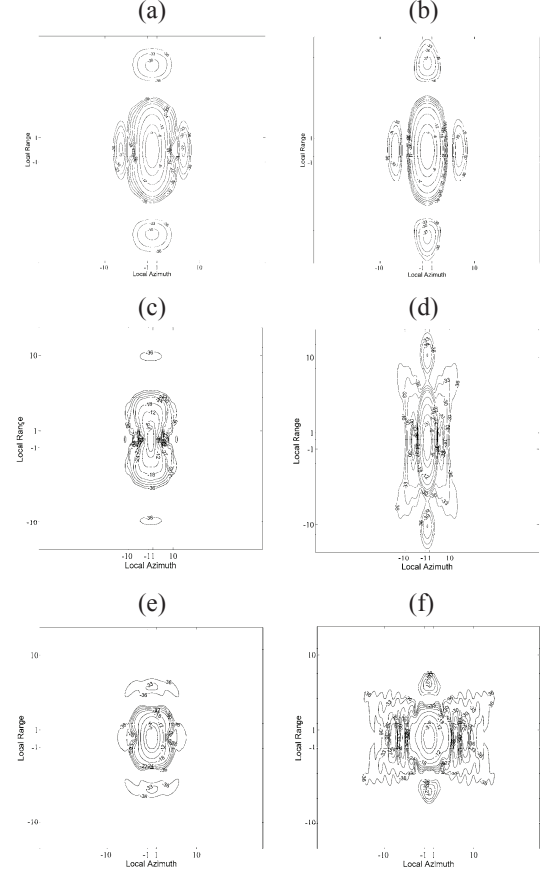


Fig. 2 SAR images of point targets generated using separable, as well as non-separable Bartlett windows. Azimuth and slant range axes are normalized with respect to -3dB-resolution of non-apodized images. Between each contour in the plot, the step is 3dB and the lowest level shown in the plot is -36dB. The images were also generated using three different choices of systems parameters. On left, the images apodized by non-separable window is shown and on the right using a separable window. In (a) and (b), system A in Table 1 was used. In (c) and (d), system B in Table 1 was used. In (e) and (f), system C in Table 1 was used.

### 3. SIDELOBE SUPPRESSION RESULTS

In order to compare the ability of the different windows to suppress sidelobes, flat spectrums were generated using

different integration angles and different relative bandwidths. After this the two-dimensional (2D) inverse Fourier transform was applied. Contour plots of the obtained amplitude SAR images are used for illustrations. In UWB SAR the shape of point targets are very different compared to that of NB SAR [6]. This may cause the normal quality measurements such as Range and Azimuth Resolution, Integrated Sidelobe Ratio (ISLR), as well as Peak Sidelobe Ratio (PSLR) to not provide useful information. For this reason, it was chosen to only show contour plots.

The resulting SAR images after apodization with  $W_{non-sep}$  and  $W_{sep}$  respectively are shown in Fig. 2. Bartlett windows were used to generate these images. Three specific values for fractional bandwidth and integration angle are selected and summarized in Table 1. The systems are all chosen to have wide integration angles and large fractional bandwidths. The parameter values are chosen in order to illustrate that with increasing integration angle and increasing fractional bandwidth, the non-separable windows gains larger advantages compared to the separable windows.

For system A the fractional bandwidth and the integration angle are large in comparison to most SAR systems, there is no remarkable difference between the use of non-separable and separable windows. However, for system B many of the new sidelobes that cannot be handled with a separable window can be suppressed with a non-separable window. For system C, it can be clearly seen that the non-separable window outperforms the separable window.

In Fig. 2, for System A, the sidelobes are in azimuth and slant range direction, as is usual in SAR images. However, for the systems B and C, sidelobes start appearing in other directions. These sidelobes are called non-orthogonal sidelobes. In [1] the non-orthogonal sidelobes are discussed, and suppressed using non-linear filtering. However, the non-separable hamming window using linear filtering has in this paper shown to be successful with regard to suppressing these sidelobes down to below -36dB.

To further evaluate the effects of non-separable windows, a further study was conducted in which Hamming windows were applied. The same parameters given in Table 1 are used again in this study, and the apodized images are shown in Fig. 3.

If we compare the images given in Fig. 2 and Fig. 3, the sidelobes are clearly lower for the point targets which were apodized by the Hamming window. This observation is the same as we expected. Comparing the sidelobe suppression ability using separable and non-separable windows, it is obvious that the non-separable windows result in lower sidelobes especially for system B and system C.

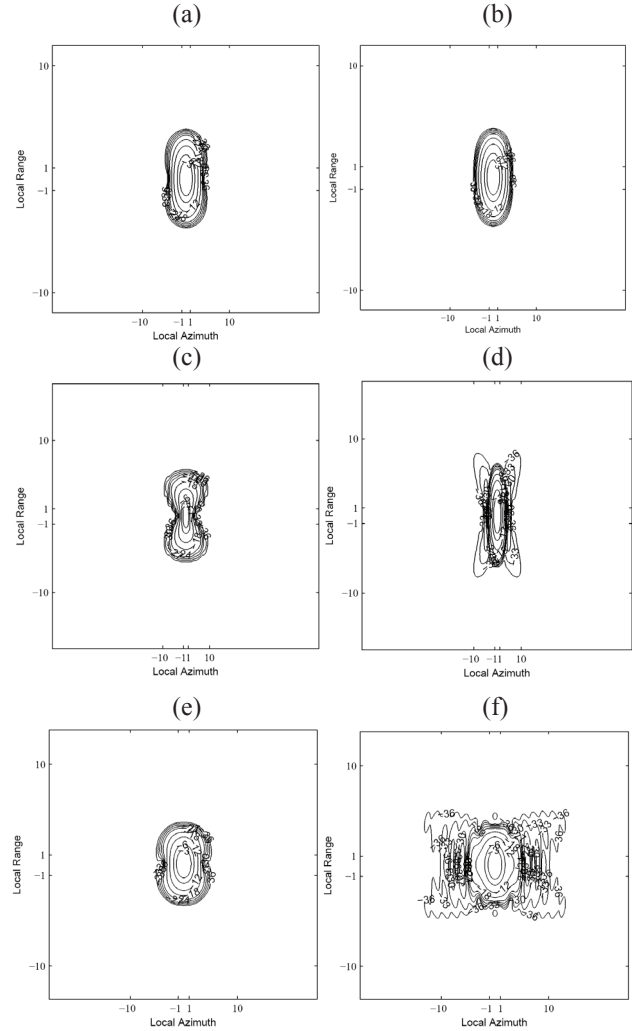


Fig. 3 SAR images of point targets generated using separable, as well as non-separable Hamming windows. Azimuth and range axes is normalized with respect to -3dB-resolution of non-apodized images. Between each contour in the plot, the step is 3dB and the lowest level shown in the plot is -36dB. The images were formed using three different choices of systems parameters. On left, the images apodized using non-separable window is shown and on the right using a separable window. In (a) and (b), system A in Table 1 was used. In (c) and (d), system B in Table 1 was used. In (e) and (f), system C in Table 1 was used. It can be observed that for the three systems under study, non-separable windows give less sidelobes compared to separable window.

#### 4. CONCLUSIONS

To conclude this paper, it has been observed that for smaller fractional bandwidths and integration angles, the difference with regard to sidelobe suppression in SAR images between applying separable and non-separable windows in the 2D wave-domain, appears very small. As the integration angle increases, non-orthogonal sidelobes appear. These non-orthogonal sidelobes can be seen both for the Bartlett and the Hamming windows. The paper also shows that using the non-separable window with both Hamming and Bartlett largely reduce the non-orthogonal sidelobes. A further increase in integration angle and in fractional bandwidth caused the improvement using non-orthogonal windows compared to orthogonal to be considerable.

#### 5. REFERENCES

- [1] V.T. Vu, T.K. Sjögren, and M.I. Pettersson, "On apodization techniques for ultra-wideband SAR imaging," *EuRAD 2009*, Rome, Italy, pp. 529-532, Sept. 30 2009-Oct. 2 2009.
- [2] H.C. Stankowitz, R.J. Dallaire, and J.R. Fienup, "Nonlinear apodization for sidelobe control in SAR imagery," *IEEE Trans. Aerosp. Electron. Syst.*, vol. 31, no. 1, pp. 267-279, Jan. 1995.
- [3] D. Pastina, F. Colone, and P. Lombardo, "Effect of Apodization on SAR Image Understanding," *IEEE Trans. Geosc. Rem. Sens.*, vol. 45, no. 11, pp. 3533-3551, Nov.2007.
- [4] X. Xu, and R.M. Narayanan, "Enhanced Resolution in SAR/ISAR Imaging Using Iterative Sidelobe Apodization," *IEEE Trans. Image Process*, vol. 14, no. 4, pp. 537-547, Apr. 2005.
- [5] J. Lim, *Two-Dimensional Signal and Image Processing*, Prentice Hall, 1990.
- [6] V.T. Vu, T.K. Sjögren, M.I. Pettersson and H. Hellsten, "An Impulse Response Function for Evaluation of UWB SAR Imaging," *IEEE Trans. Signal Process*, vol. 58, no. 7, pp. 3927-3932, July. 2010.